Kinetics of thermally induced processes in Ag doped $As_{40}Se_{30}Te_{30}$ chalcogenide glass

R. Vigi[a], G. R. Štrbac[a], D.D. Štrbac[b,*], O. Bošák[c], M. Kubliha[c]
[a]*University of Novi Sad, Faculty of Sciences, Trg Dositeja Obradovica 4, Novi Sad, Serbia*
[b]*University of Novi Sad, Faculty of Technical Sciences, Trg Dositeja Obradovica 6, Novi Sad, Serbia*
[c]*Faculty of Materials Science and Technology, Slovak University of Technology, Bottova 25, 917 24 Trnava, Slovakia*

The processes of glass-transition and crystallization of chalcogenide glass $As_{40}Se_{30}Te_{30}$ with 5 at.% silver were analyzed using differential scanning calorimetry. The values of glass-transition temperatures and activation energy were determined. Two crystallization processes were also detected and three-dimensional growth. Using non-isoconversional models the activation energies for both processes amounted to 112(2) kJ/mol and 97(2) kJ/mol. Isoconversional models were used to track changes in activation energy. The presence of Te significantly affects the thermal parameters as well as the structure of the glass while the presence of Ag does not significantly change the degree of connectivity of the $As_{40}Se_{30}Te_{30}$ glass matrix.

(Received October 20, 2023; Accepted January 4, 2024)

Keywords: Amorphous materials, Phase transition, Crystallization kinetics, Thermal analysis

1. Introduction

Chalcogenide glasses from the As-Se-Te system, recently gained attention, especially to their simple synthesis and chemical stability, but also due to their unique physical properties and potential use in various modern technologies such as phase-changing memories, infrared and fiber optics [1-5].

Se-based glasses are well known for their properties attractive for applications in electronics and optics [6,7], while the addition of Te in glass is proven to increase corrosion resistance and reduce band gap [8]. Chalcogenide glasses can easily be doped with silver and it can be done with high content. Introducing silver in amorphous matrix can alter their electrical and thermal properties. This effect can be crucial for their applications in many areas of modern technology, such as phase change memories (PCM), in which the transition from amorphous to crystalline state occurs and it is characterized by large changes in electrical conductivity, whereby the study of crystallization processes and the behaviour of materials during heating is imposed as the basis of material characterization [9,10].

The study of thermally induced crystallization and glass transition processes provides an insight into the structure of the glasses and the given processes, thereby enabling a better understanding of interdependence of glass structure and experimentally detected macroscopic physical and chemical properties. In this sense, these glasses are particularly interesting for research since the matrix itself contains a large number of different structural units [11].

For the reasons stated above, this paper was done with the aim of studying the process of glass transition and crystallization in the selected composition of Ag-doped chalcogenide glass with the $As_{40}Se_{30}Te_{30}$ matrix, and determining the correlations between composition, structure and experimentally detected thermal characteristics.

*Corresponding author: draganastrbac@uns.ac.rs
https://doi.org/10.15251/CL.2024.211.21

Various theoretical models have been developed for the crystallization and glass transition kinetics and activation energy of these processes. In this paper, a system with 5at.% of silver was investigated by using two different approaches, non-isoconversional and isoconversional.

A system with 5at.% of silver was investigated by using three different non-isoconversional models: Kissinger [12,13],Mahadevan [14], and Augis-Bennett [15], and three different isoconversional models: Vyzovkin [16,17], Kissinger-Akahira-Sunose [18], Ozawa-Flynn-Wall [19]. The Johnson-Mehl-Avrami model was used to detect the type of nucleation and crystal growth mechanism [20-23]. Also, three different models were used for analysing the glass transition process, based on the influence of heating rate on the glass transition temperature.

2. Experimental

The glass was synthesized from high-purity elementary components (at least 99.99 %). The weighted elements in a total of 12 g were loaded into cleaned quartz tubes and then sealed under a vacuum using an acetylene/oxygen torch. Masses were measured by analytical balance METTLER B-6 with an accuracy of $\pm 5 \cdot 10^{-8}$ kg. For the synthesis of the glass with the desired composition, the classical method of cascade heating and air-quenching was used. The maximum temperature of the synthesis was 950 °C, at which the sample was maintained for 5 hours and then quenched in the air in order to preserve the structure that corresponds to the structure of the melt at the maximum synthesis temperature. A sufficiently high cooling rate prevents the structural elements from rearranging in accordance with the spatial distribution of the dominant chemical bonds and thus forming a crystalline, ordered state. After quenching, the tube is placed in Al_2O_3 powder to minimize quench-related stress in the material.

XRD measurements were conducted on RigakuMiniFlex 600 instrument, with CuK_α radiation. All synthesized glasses were checked for unwanted crystallization by using the X-ray diffraction (XRD) measurements in angle interval from $2\theta = 20 - 70^\circ$ .The second XRD measurement was conducted after annealing at crystallization temperature to detect and identify the crystalline phases formed within the sample.

The SEM observations were performed by using a JEOL JSM 7600F (JEOL Ltd., Tokyo, Japan) scanning electron microscope (SEM) equipped with an Energy Dispersive Spectrometer (EDS), operating at an acceleration voltage of 20 kV. Amorphous samples as well as samples after annealing were coated by conducting gold layer before a microscopic observation.

Thermal properties, primarily those related to glass transition and crystallization processes were determined by the use of differential scanning calorimetry (DSC). Measurements were conducted by using a Mettler Toledo DSC 822e. Nitrogen was used as the purge gas at a rate of 100 ml/min. The calorimeter was calibrated through measurements of the melting processes of In and Zn. About 10 mg of the sample were measured in powder form and sealed in a 100µl aluminium pan. Non-isothermal DSC curves were obtained at selected heating rates of 5, 7, 10, 12, 15, 20, 25, and 30 K/min in the range of 343-673 K.

3. Results and discussion

The $As_{40}Se_{30}Te_{30}$matrix was chosen since it is located deep in the glass formation region in the As-Se-Te system [24].This enables obtaining of amorphous samples without extreme cooling conditions, and therefore without high stresses within the obtained new materials. The diffractogram shown in Fig. 1, does not contain any sharp diffraction peaks above the baseline and thus confirms the amorphous character of the sample. Two broad diffraction bands are clearly observed at about $2\theta = 30^\circ$ and 50°. They arise from the short-range (mostly nearest neighbour) covalently networking structures. Those two peaks are also ofaweak intensity, with a small relative number of counts and therefore, they are not a consequence of the existence of a crystal phases.

Fig. 2 shows SEM image of the obtained sample with the marked area on which the EDX area scan was performed. Table 1 provides data on the composition of the sample based on the

EDX area scan. This scan showed that the composition of the sample roughly matches the targeted composition.

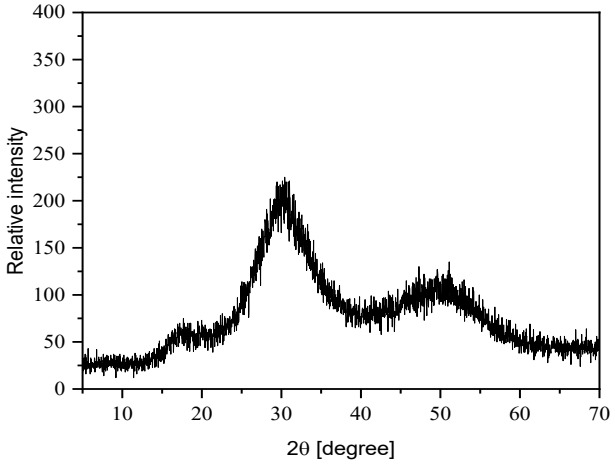

Fig. 1.XRD pattern of as-synthesized $Ag_5(As_{40}Se_{30}Te_{30})_{95}$.

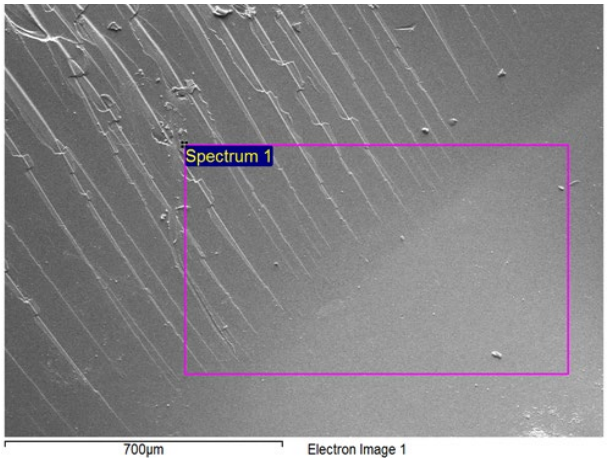

Fig. 2.SEM image with EDX area scan in the amorphous sample.

Table 1.The sample composition based on the EDX area scan.

Element	As	Se	Ag	Te
Content [at.%]	35.95	34.29	4.20	25.56

Fig. 3 shows the DSC curves of the synthesized sample, at different heating rates. Three regions can be observed on the obtained DSC curves, the first endothermic process at 403 K is the glass-transition region, the second at around 493 K is the exothermic process of crystallization, which is complex and consists of two peaks. In the third region, at 573 K a complex melting process can be observed, which also consists of two peaks.

DSC curves show that the glass-transition process shifts to higher temperatures with an increase of the heating rate, as well as in the case of both crystallization peaks. These two crystallization peaks are better separated with an increase of the heating rate in the experiment. For the purposes of this work and the calculation of the crystallization activation energy, the deconvolution of the peaks was performed.

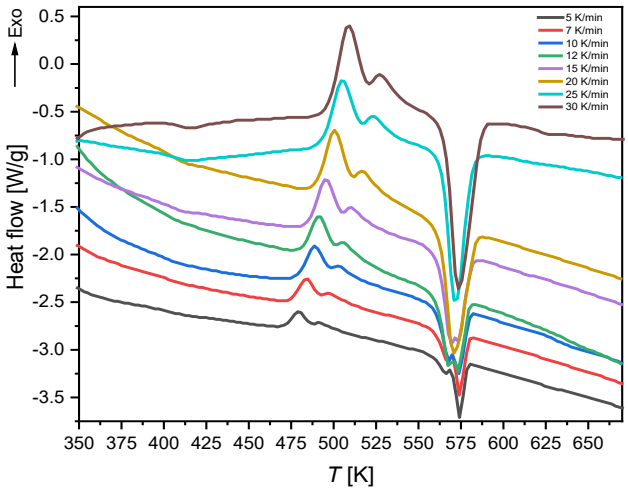

Fig.3. DSC curves of $Ag_5(As_{40}Se_{30}Te_{30})_{95}$ using different heating rates.

3.1. Glass-transition process

The glass-transition process represents a basic thermally induced process in glasses, closely related to their structure and properties. Two parameters are most often used for its quantification: glass-transition temperature, T_g and apparent activation energy, E_g. Glass-transition temperature characterizes the rigidity and strength of glass materials and depends on the nature of the material itself, the method of analysis, and the applied heating rate. Above the glass-transition temperature, the system is in the rubbery state and bellow T_g, the system is in the glassy/hard state. Fig.3showsthat the glass-transition of the $Ag_5(A_{s40}Se_{30}Te_{30})_{95}$sample is of a very low thermal effects and for this reason, it was not possible to do an isoconversional analysis of this thermal phenomenon. Also, the glass-transition process of such low intensity may indicate that this type of glass is very stable and close to its thermodynamic equilibrium and does not undergo significant configuration transformations during this process. The glass-transition phenomena will be discussed on the basis of three models: Lasocka, Kissinger and Moynihan.

Lasocka's empirical relation (1)[25] shows that there is a linear dependence between the applied heating rate β and the value of the glass-transition temperature T_g:

$$T_g = A + B \ln \beta \tag{1}$$

Where A represents the glass-transition temperature at a heating rate of 1 K/min, while the slope on the heating rate is characterized by parameter B. The significance of this parameter is that it indicates configurational changes during the glass-transition process, and its value enables the comparison of these changes with different compositions [25].

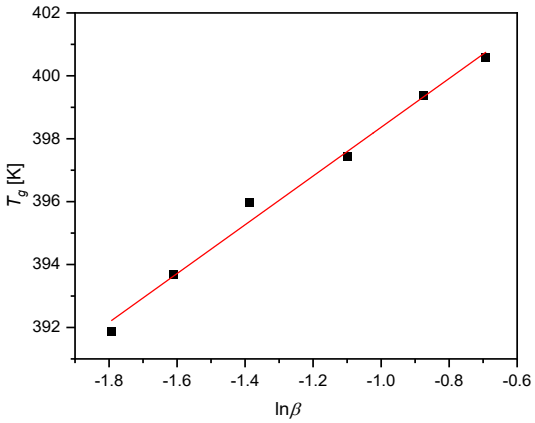

Fig.4.Dependence of T_g on β fitted with the Lasocka model.

Fig. 4 graphically shows the dependence of the glass-transition temperature on the applied heating rate fitted with the Lasocka model. A good linear dependence indicates that the synthesized samples follow the empirically predicted dependence. Calculated parameter *A*, the glass-transition at a heating rate of 1 K/s, is 406.1(5) K ,while calculated value of *B*, which defines the time response of configurational changes in the material in the glass-transition region, is 7.8(4).

By comparing the obtained value of *B* with the composition containing S instead of Te in the matrix (*B*=4.5(5) [26]), it can be concluded that the introduction of tellurium leads to a significant increase in this parameter, indicating an increase in changes during the glass-transition process. On the other hand, compared to the matrix itself, without silver, (*B*=7.33 [11]) the introduction of silver into the matrix does not lead to significant changes in the value of parameter *B*. Accordingly, parameter *A* shows a significant decrease when replacing S with Te [26], that is, in comparison with the matrix itself, it shows a slight increase [11].

Kissinger model is one of the most commonly used models for determining the activation energies in thermally induced processes in all kinds of materials. The problem that can appear when this model is being used is that it gives a single value of the apparent activation energy of crystallization, overlooking the often present complexity of the thermally stimulated processes. Kissinger model in its simplest form can be written as:

$$\ln\left(\frac{\beta}{T_g^2}\right) = -\frac{E_g}{RT_g} + const. \tag{2}$$

Where *R* is the gas constant.

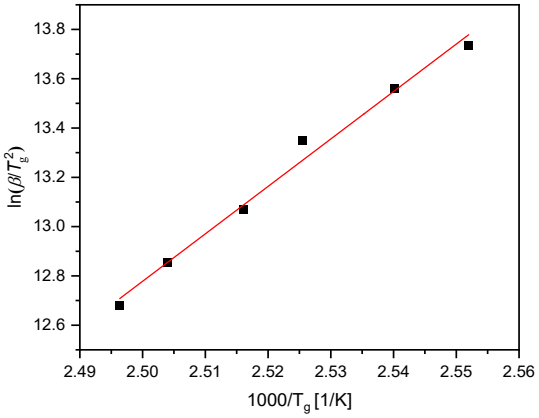

Fig.5.Dependence of $\ln\left(\frac{\beta}{T_g^2}\right)$ *on* $\frac{1000}{T_g}$ *fitted with the Kissinger mode.l*

Fig. 5 shows the dependence of $\ln\left(\frac{\beta}{T_g^2}\right)$ on $\frac{1000}{T_g}$ fitted with the Kissinger model and the obtained value of the activation energy is given in Table 2.

Moynihan model is also a frequently used model for determining of glass-transition activation energy. The activation energy is determined from the dependence (3):

$$\ln(\beta) = -\frac{E_g}{RT_g} + const. \tag{3}$$

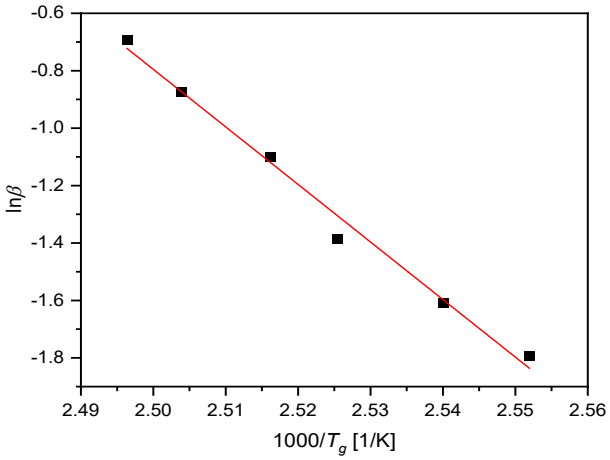

Fig. 6.Dependence of $\ln(\beta)$ *on* $\frac{1000}{T_g}$ *fitted with the Moynihan mode.l*

Fig. 6 shows the Moynihan model for determining the activation energy. Glass-transition region and activation energies for the glass-transition were analysed by using two different approaches, Kissinger and Moynihan, and were found to be 160(3) kJ/mol and 167(3)kJ/mol, respectively. This indicates that both models can successfully be used for calculating glass-transition energies. Similar recent studies of glass-transition activation energies [11] showed that E_g for the $As_{40}Se_{30}Te_{30}$matrix corresponds to the obtained results of the composition doped with silver in this paper. This indicates that introduction of silver in the percentage of 5 at.% does not lead to a change in glass-transition activation energy, which is in accordance with the results obtained by use of the Lasocka model. It can be concluded that the introduced silver does not influence the material's ability to transit from the metastable state to the state with minimum energy. By comparing the obtained values with the values for the analogous glass which contains identical share of silver, but has sulphur in the matrix instead of tellurium [26], one can conclude that tellurium in glass significantly lowers the value of the activation energy.

Table 2. Values of the glass-transition temperature, parameters A and B, and glass-transition activation energies E_g fitted for non-isoconversional models.

Glass composition	β [K/min]	T_g [K]	A [K]	B [K]	E_g [kJ/mol] Kissinger	E_g [kJ/mol] Moynihan
$Ag_5(As_{40}Se_{30}Te_{30})_{95}$	10	391.9	406.1(7)	7.8(6)	160(3)	167(3)
	12	394.0				
	15	396.0				
	20	397.4				
	25	399.4				
	30	400.6				

*T_g for the heating rate of 5 and 7 K/min were impossible to read with sufficient precision.

Changes caused by the introduction of tellurium instead of sulphur in the matrix can be explained primarily by structural changes. The glass network in Ag-($As_{40}S_{30}Se_{30}$) consists of three-dimensional As_2S_3 and As_2Se_3 units, while when replacing sulphur with tellurium in the network As_2Te_3 chain-like structure appears. This results in the glass having a chain-like layered structure, made up of bi-coordinated selenium and tellurium atoms instead of a three-dimensional structure. This matrix is additionally stabilized by Van der Waals bonds between chain structures, which lead to a decrease in T_g [11]. Certainly, the strength of the chemical bonds also exerts an additional influence, since tellurium has a lower electronegativity.

The introduction of 5 at.% of silver in the $As_{40}Se_{30}Te_{30}$ matrix does induce the change in activation energy, while the same silver content in the $As_{40}S_{30}Se_{30}$ matrix causes a significant shift of this quantity, indicating a formation of different structural units.

3.2. Crystallization

Crystallization kinetics in amorphous chalcogenides can be investigated by isoconversional and non-isoconversional methods. As already said and as can be seen from the obtained DSC curves (Fig. 3), the crystallization process is complex and consists of two crystallization peaks that overlap to a certain extent. Therefore it is necessary to perform deconvolution of the peaks for their further analysis (Fig. 7).

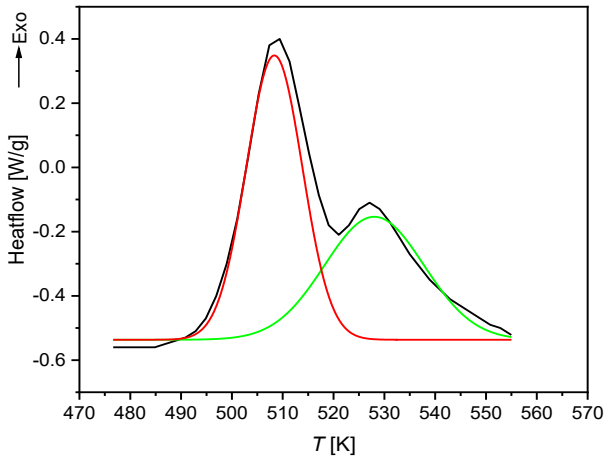

Fig. 7. Deconvoluted crystallization peaks from DSC curves, example for heating rate 30 K/min.

In order to determine the structural units that crystallize, crystallization processes were induced. The sample was annealed according to DSC measurements at a 10 K/min heating rate and held ata crystallization temperature of 501 K for one hour. The sample prepared in this way was then characterized by using XRD diffraction and the peaks indicating the crystallized structural units were identified.

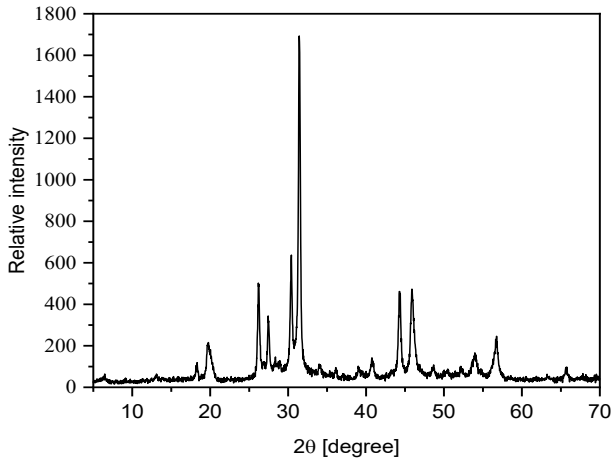

Fig.8.XRD pattern of annealed $Ag_5(As_{40}Se_{30}Te_{30})_{95}$.

The XRD peaks of the annealed sample can be observed in Fig.8. The diffraction maxima are assigned to the corresponding structural units and were indexed by using the International Centre for Diffraction Data (ICDD) files. Identified structural units are As_2Se_3 (26-0123) and $AsSe_{0.5}Te_{0.5}$ (37-1124) matrix structural units and $AgAsSe_2$ (30-1130), which is in agreement with previously published papers [27]. The presence of those exact structural units is also confirmed by the melting temperatures on the obtained DSC curves.

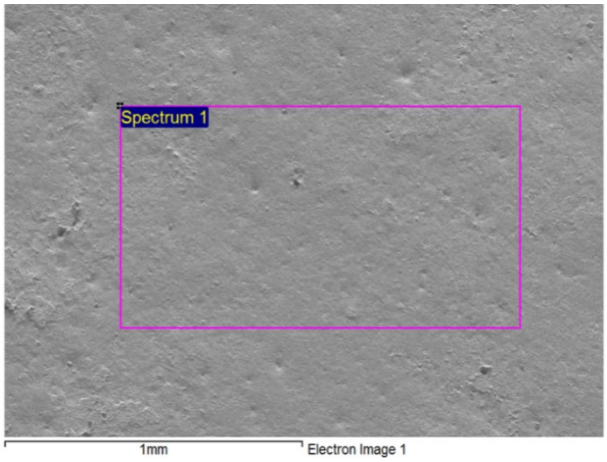

Fig.9.SEM images with EDX area scan of the annealed sample.

Table 3.The annealed sample composition based onthe EDX area scan.

Element	As	Se	Ag	Te
Content [at.%]	32.04	37.45	5.80	24.71

EDX area scan of the annealed sample showed that the composition of the sample approximately matched the targeted composition (Table 3).The differences between the targeted composition of the synthesized sample and the EDX measurements probably originate from the error in determining the proportion of As and Se due to the similar values of their atomic masses.

3.2.1. Johnson-Mehl-Avrami model

Crystallization kinetic analysis is usually carried out by using the classical theoretical model developed by Johnson, Mehl and Avrami (JMA model). Due to simplicity, this model is widely used to describe the evolution of the crystallization process in terms of the crystallized fraction (extent of conversion) as a function of time (χ) [20-23]:

$$\chi = 1 - \exp\left(-Kt^{n}\right) \tag{4}$$

Where K is a rate constant determined by the nucleation and growth rates, and n is the Avrami exponent which describes the crystal growth dimensionality. JMA parameters were fitted on the basis of optimal percentages of crystallization at differentheating rates. Points with extent of conversion below 0.5 and over 99 % were not taken into account due toa high error.

According to JMA model, the mechanism of nucleation and crystal growth determines the shape of the exothermic peak and is described by the relation:

$$\ln\left(-\ln\left(1-\chi\right)\right) = -n\ln\beta - \frac{1.052mE_c}{RT} + const. \tag{5}$$

n and m are numerical factors depending on morphology and growth of crystalline nuclei and E_c is apparent activation energy of crystallization.

The ratio of the parameters n and m is determined by the crystallization process in the sample itself, by the type of nucleation and the evolution of crystallization during the heating of the sample.

Unlike other methods that are based on the position of the maximum of the crystallization peak, this one also takes into account the analysis of the shape of the peak itself. The practical application of this relation to the results of DSC measurements consists in keeping one of the three parameters (χ, β, T) constant, while the parameters n, m and E_c are determined from the linear dependence (predicted by relation 5). Figs. 10-12 graphically present these procedures for both crystallization peaks. Due to the significant shift of the crystallization peaks on the temperature scale with the increase of the applied heating rate and the fact that too low and too high values of the degree of crystallization are not representative for fixed temperatures, only four heating rates were taken, especially for the lower and especially for the higher applied rates.

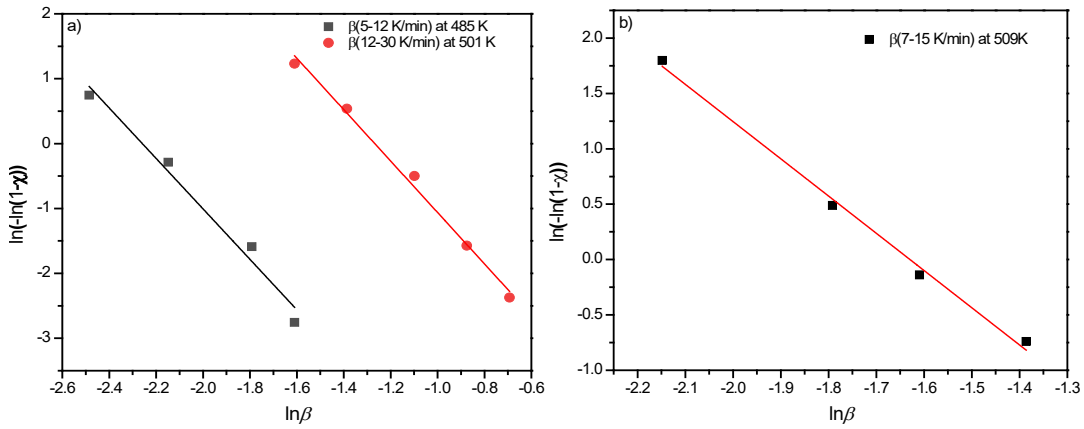

Fig.10. Plots of $\ln(-\ln(1-\chi))$ *vs.* $\ln(\beta)$ *fitted with the JMA model:a) first peak and b) second peak.*

The slope of the linear dependencies shown in Fig. 10, according to relation (5), corresponds to the parameter *n*, estimated to be 3.87 for the first peak and 3.36 for the second peak.

Parameter *m* can be calculated from JMA model (Fig. 11), since according to relation (5) for a fixed χ the slope of the linear dependence is $\frac{1.052mE_c}{Rn}$. Value of *m* is estimated to be 3.93 for the first peak and 3.42 for the second peak.

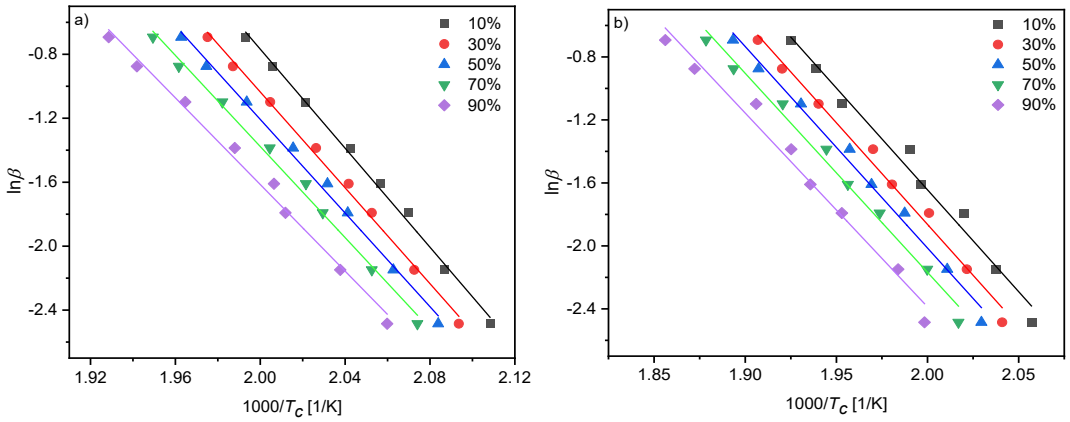

Fig.11. Plots o f $\ln(\beta)$ *vs.* $\frac{1000}{T_c}$ *at various conversions, fitted with the JMA model: a) first peak and b) second peak.*

Deviations from the expected linear dependencies for a fixed applied heating rate, which can be seen from the graphs shown in Fig. 12, indicate that there is a small change in the activation energy during the crystallization process itself. Quantitative change of this parameter will be analysed within isoconversion approaches. A rough estimate from these dependencies confirms the values of *m* and *n* parameters. The parameter values themselves indicate that volume nucleation with three-dimensional growth is present in both crystallizations, with the difference that at the first crystallization peak, the number of crystallization centres changes during the process.

3.2.2. Non-isoconversional models

Determining the activation energy of the crystallization process is possible based on the analysis of the temperature change that corresponds to the maximum of this exothermic process with the applied heating rate. On this basis, the Kissinger, Mahadevan, and Augis-Bennett models were developed. The first two models are based on the previously mentioned relations (3) and (4), with the difference that instead of the glass-transition temperature T_g, the temperature corresponding to the maximum of the crystallization peak, T_c appears. The corresponding fits according to the Kissinger and Mahadevan models are shown in Figs. 13 and 14, respectively, while the values of the calculated apparent activation energies of crystallization are given in Table 4.

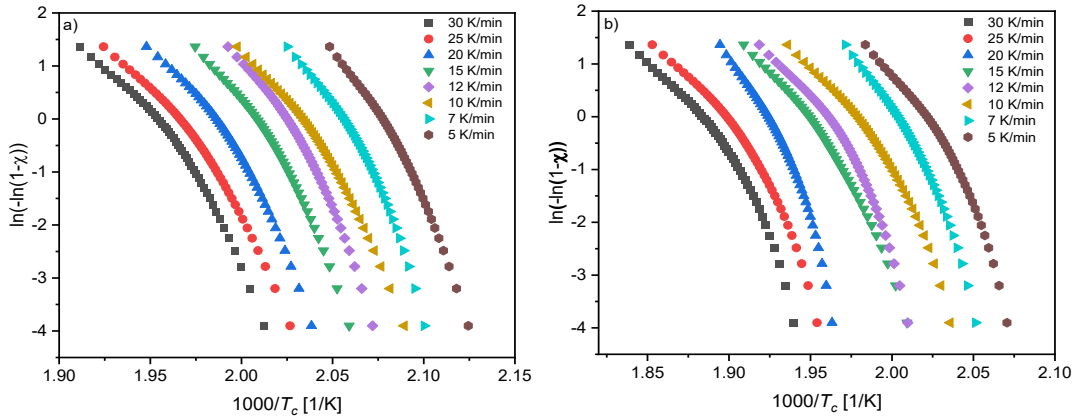

Fig. 12. Plots of $\ln(-\ln(1-\chi))$ *vs.* $\frac{1000}{T_c}$ *at various heating rate: a) first peak and b) second peak.*

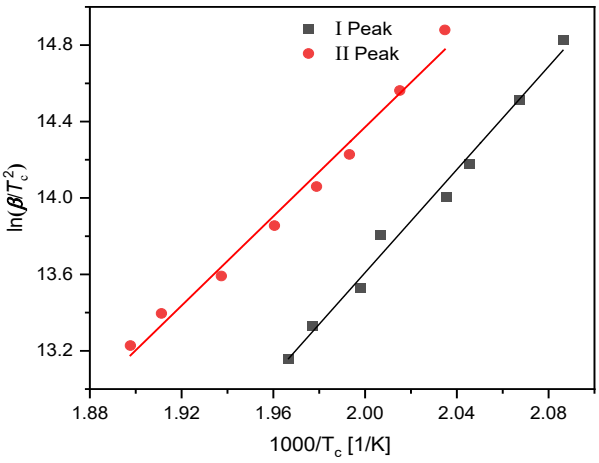

Fig.13. Plots o f $\ln\left(\frac{\beta}{T_c^2}\right)$ *vs.* $\frac{1000}{T_c}$ *fitted with the Kissinger model.*

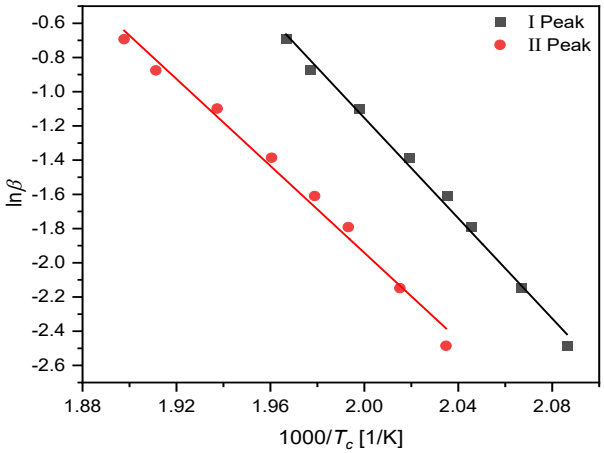

Fig.14. Plots of $\ln(\beta)$ *vs.* $\frac{1000}{T_c}$ *fitted with the Mahadevan model.*

Augis-Bennet is a non-isoconversional model that can be used to describe crystallization activation energies in glasses. In its logarithm form can be expressed as:

$$\ln\left(\frac{T_c - T_0}{\beta}\right) \approx \frac{E_c}{RT_c} - \ln K_0 \tag{6}$$

Where T_c and T_0 are the crystallization peak temperature and starting temperature of the experiment, respectively, R is the universal gas constant, and K_0 is a crystallization frequent factor [15]. Fig. 15 shows dependence of $\ln\left(\frac{T_c - T_0}{\beta}\right)$ on $\frac{1000}{T_c}$.

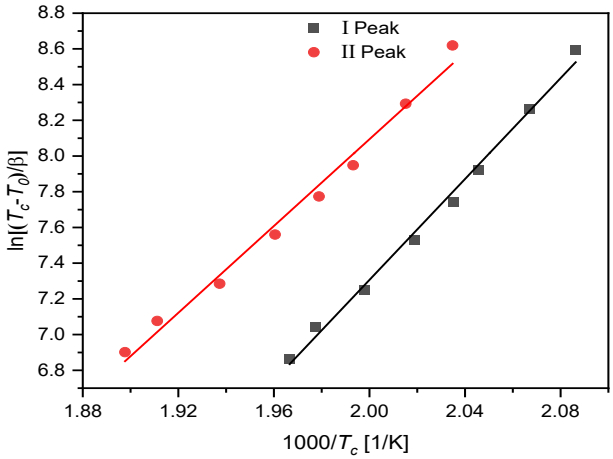

Fig. 15. Plots of $\ln\left(\frac{T_c - T_0}{\beta}\right)$ *vs.* $\frac{1000}{T_c}$ *fitted with the Augis-Bennet model.*

The results in Table 4 show that calculated crystallization activation energies for all three non-isoconversional models are similar, which means that all three models describe the crystallization process equally well, and that analysis of the crystallization process of other silver-doped chalcogenide glasses [11, 28] are in agreement with the obtained results. These models characterize the crystallization process by a single value of apparent activation energy. In order to examine the complexity of the crystallization process, i.e. the change of this parameter during the process itself, isoconversional methods were also applied.

Table 4.Calculated crystallization activation energies.

Model	E_c [kJ/mol]	
	Peak 1	Peak 2
Kissinger	112.1(22)	97.1(21)
Mahadevan	121.8(20)	105.6(22)
Augis-Bennet	117.5(20)	101.1(21)

3.2.3. Isoconversional models

Vyazovkin model is a flexible integral method where activation energy is found at the minima of function:

$$\Phi(E_\chi) = \sum_{i=1}^{n} \sum_{j \neq i}^{n} \frac{I(E_\chi, T_{\chi,i})\beta_j}{I(E_\chi, T_{\chi,j})\beta_i} \tag{7}$$

which represents the activation energy for a given conversion percentage. As solving the integral $I(E_\chi, T_\chi)$ is complex both from the aspect of mathematics and the aspect of the physical process it describes, the well-known approximation of Gorbachev approximation [29] is used for its solution:

$$I(E_\chi, T_{\chi,i}) = \int_0^{T_\chi} e^{-\frac{E_\chi}{RT}} dT = \frac{RT_\chi^2}{E_\chi + 2RT_\chi} e^{-\frac{E_\chi}{RT}} \tag{8}$$

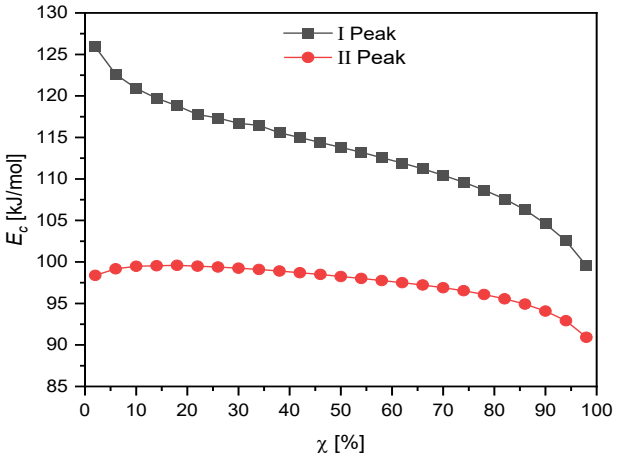

Fig. 16. Plotsof $E_c$vs χ fitted with the Vyzovkin model.

Fig. 16 shows the results obtained by using the Vyazovkin model. These results show a slight decrease in the crystallization activation energy for the first crystallization process, while for the second process, the energy obtained by this model is almost constant for different extents of crystallization.

KAS model is the linear isoconversional method developed using Coats and Redfern approximation [18]. In general the KAS model establishes a connection between the heating rate and the temperature at which the corresponding extent of crystallization.

$$\ln\left(\frac{\beta}{T_\chi^2}\right) = -A\frac{E_\chi}{RT_\chi} + const. \tag{9}$$

Fig. 17 shows linear dependencies according to relation 9 for both crystallization peaks and for five selected extents of crystallization.

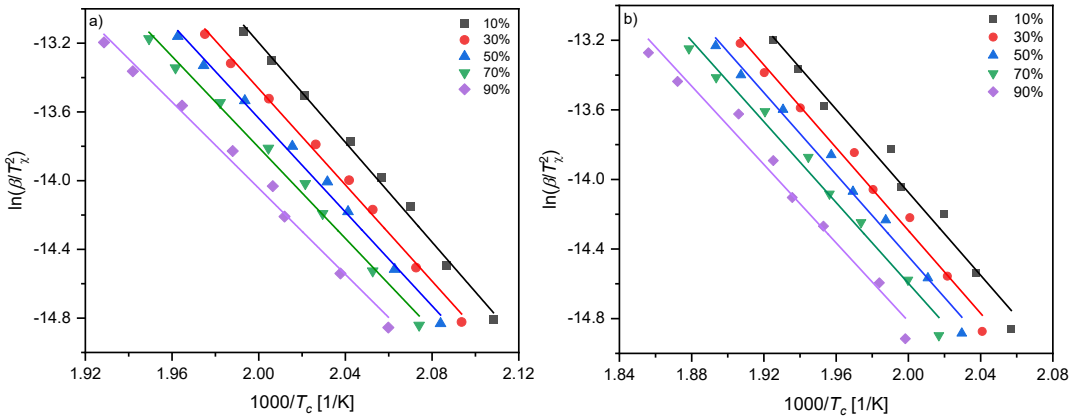

Fig. 17.Plots of $\ln\left(\frac{\beta}{T_\chi^2}\right)$ *vs* $\frac{1000}{T_c}$ *fitted with the KAS model: a) first peak and b) second peak.*

OFW model is an isoconversional method for determining of activation energies of crystallization using Doyle approximation [19], the final form of this model can be represented as:

$$\ln(\beta) = -1.0516\frac{E_\chi}{RT_{\chi,i}} + C_{OFW} \tag{10}$$

Fig. 18 presents the plots obtained by applying the OFW model to the experimental results obtained from DSC measurements.

Table 5 shows the calculated crystallization activation energies obtained by using different isoconversional models. The results show good agreement between the obtained values. Also, the obtained results are in agreement with the results [11] where the $As_{40}Se_{30}Te_{30}$ matrix was examined. If the activation energies of non-isoconversional models and isoconversional models for $\chi = 0.5$ are compared, it can be noted that they also agree to a certain extent. Small changes in the value of this parameter justify the application of the JMA model for characterizing the way of crystallization of structural units.

Activation energies obtained by using three different isoconversional models for the first peak decrease with a higher extent of crystallization, indicating that the crystallization process is a complex, multi-stage process, which includes several mechanisms and processes of crystal growth in an amorphous sample. As the application of the JMA model has already shown for this crystallization process, the number of crystallization centres changes during the process itself.

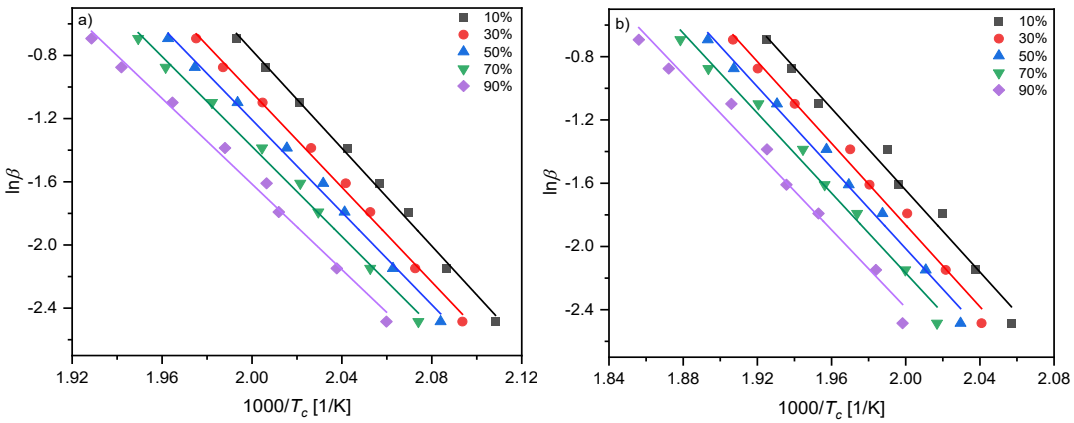

Fig. 18.Plots of $\ln(\beta)$ *vs* $\frac{1000}{T_\chi}$ *fitted with the OFW model: a) first peak and b) second peak.*

Table 5. Crystallization activation energies in kJ/mol at different percentages of crystallization for calculated models.

χ \ Model		E_c [kJ/mol]		
		KAS	Vyazovkin	OFW
10	I Peak	120.6(18)	120.9	122.4(18)
	II Peak	99.1(24)	99.5	102.2(24)
30	I Peak	116.43(18)	116.7	118.5(18)
	II Peak	98.9(21)	99.2	102.1(21)
50	I Peak	113.5(18)	113.8	115.8(18)
	II Peak	97.91(20)	98.2	101.2(20)
70	I Peak	110.2(19)	110.4	112.6(19)
	II Peak	96.5(21)	96.9	99.9(21)
90	I Peak	104.3(21)	104.6	107.1(21)
	II Peak	93.7(24)	94.1	97.3(24)

4. Conclusion

In this work, the significant thermal characteristics of chalcogenide glass with the composition $Ag_5(As_{40}Se_{30}Te_{30})_{95}$ were analysed by using the DSC method at different heating rates. Thermally induced crystallization and glass-transition processes were analysed by using different models.

First, the amorphous character of the synthesized glass was confirmed by the XRD method, while it was additionally confirmed by SEM images. EDX area scan confirmed that the composition of the obtained sample roughly matches the targeted composition.

For the glass-transition process, it was shown that it is a small exothermic process, so that the glass does not suffer major configurational changes during the process itself. The glass-transition temperatures and activation energies for this process were determined as the two most important parameters and their values are: T_g=391.5(5) K at a heating rate of 10 K/min and E_g=160(3) kJ/mol.

The crystallization process consists of two exothermic maxima. The application of the JMA model to these two processes showed that the first process is characterized by parameter values of n~3.87, which indicates a volume nucleation and three-dimensional growth with a variable number of centres, while the value for the second crystallization peak is n~3 and it indicates the same crystallization mechanism but with a constant number of centres.

The activation energy value for the first crystallization process is slightly higher (E_c=112(2) kJ/mol according to Kissinger's model) compared to the second crystallization process E_c=97(2) kJ/mol.

Using isoconversion models, it was shown that in the case of the first crystallization process, there is a drop in the value of the activation energy during the process itself, which confirms that it is a complex process, as indicated by the JMA model. The activation energy of the second process remains approximately constant. The results of all applied models showed their good consistency.

In addition to the quantitative values of the physical parameters that characterize the examined processes, some very interesting qualitative results were also obtained by applying the mentioned methods and analyses. First, the comparison of the obtained results with the results for the analogous composition with S instead of Te indicates a significantly different structure of the glass and the degree of connection of the glass network. The structure of the examined glass is most likely characterized by a chain-like layer structure, and it is additionally stabilized by Van

der Waals bonds between the chains. On the other hand, it was shown that the introduction of silver into the given matrix in the investigated percentage minimally affects the degree of connection of the glass matrix and its thermodynamic stability.

Acknowledgments

The authors acknowledge financial support of the Provincial Secretariat for Higher Education and Scientific Research (Project: Novel chalcogenide materials for efficient transformation and use of energy). This work has been also supported by the European Regional Development Fund under contract No. ITMS2014+: 313011W085. The authors acknowledge Prof. Dr Srdjan Rakic for XRD measurements.

References

[1]K. Gmucova, J. Mullerova,Amorphous materials, Nova Science Publishers Inc, pp.1 (2013)
[2]P. Noé, C. Vallée, F. Hippert, F. Fillot, J.Y. Raty, Semiconductors Science and Technology **33**(1), 013002(2018);10.1088/1361-6641/aa7c25
[3]A.Z. Mahmoud, M. Mohamed, S. Moustafa, A.M. Abdelraheem, M. A. J.Abdel-Rahim,Journal of Thermal Analysis and Calorimetry **131**(3), 2433 (2017);10.1007/s10973-017-6793-3.
[4]M.S. Kamboj, G. Kaur, R. Thangaraj, Thin Solid Films **420/421**, 350 (2002);10.1016/S0040-6090(02)00848-9
[5]A. Sherchenkov, S. Kozyukhin, A. Babich,Journal of Thermal Analysis and Calorimetry **117**(3), 1509 (2014);10.1007/s10973-014-3899-8
[6]P. Yadav, A. Sharma, Phase Transitions, **88**(2), 109 (2014);10.1080/01411594.2014.961152
[7]A.A. Joraid, A.A. Al-Marweny, M.A. Al-Maghrabi, Journal of Thermal Analysis and Calorimetry **147**(5), 3633 (2021);10.1007/s10973-021-10790-7
[8]E. Shaaban, Y.A. Ismail, H.S. Hassan, Journal of Non-Crystalline Solids**376,**61 (2013);10.1016/j.jnoncrysol.2013.05.024
[9]G.R. Štrbac, J.S. Petrović, D.D. Štrbac, K. Čajko, S.R. Lukić-Petrović, Journal of Thermal Analysis and Calorimetry**134**(1), 297 (2018);10.1007/s10973-018-7151-9
[10]M. Mohamed, M.N. Abd-el Salam, M.A. Abdel-Rahim, A.Y. Abdel-Latief,E.R. Shaaban,Journal of Thermal Analysis and Calorimetry**132**(1), 91 (2017);10.1007/s10973-017-6873-4
[11]V.S. Shiryaev, J.L. Adam, X.H. Zhang, M.F. Churbanov, Solid State Sciences **7**(2), 209 (2005);10.1016/j.solidstatesciences.2004.10.027
[12]H.E. Kissinger, Journal of Research of the National Bureau of Standards**57**, 217 (1956);10.4236/gep.2021.96004
[13]H. E. Kissinger, Analytical Chemistry**29**, 1702 (1957);10.1021/ac60131a045
[14]S. Mahadevan, A. Giridhar, A. K. Singh,Journal of Non-Crystalline Solids**88**, 11 (1986);10.1016/S0022-3093(86)80084-9
[15]J.A. Augis, J.E. Bennett,Journal of Thermal Analysis and Calorimetry**13**, 283 (1978);10.4236/jamp.2017.58127
[16]S. Vyazovkin, Journal of Computational Chemistry **18**, 393 (1997);10.1002/(SICI)1096-987X(199702)18:3<393::AID-JCC9>3.0.CO;2-P
[17]S. Vyazovkin, Journal of Computational Chemistry**22**, 178 (2001);10.1002/1096-987X(20010130)22:2<178::AID-JCC5>3.0.CO;2-%23
[18]T. Akahira, T. Sunose, Research Report, Chiba Institute of Technology**16**, 22 (1971);10.4236/ijcm.2020.112002
[19]J. Opfermann, E. Kaisersberger, Thermochimica Acta **203**, 67 (1992);10.1016/0040-6031(92)85193-Y
[20]W. A. Johnson, K.F. Mehl, Transactions of the American Institute of Mining and Metallurgical Engineers**135**, 416 (1939);10.4236/jcpt.2016.64004
[21]M. Avrami,Journal of Chemical Physics **7**(12), 1103 (1939);10.1063/1.1750380

[22]M. Avrami,Journal of Chemical Physics **8**(2), 212 (1940);10.1063/1.1750631
[23]M. Avrami, Journal of Chemical Physics**9**(2), 177 (1941);10.1063/1.1750872
[24]G.Z. Vinogradova,Glass formation and phase equilibrium in chalcogenide systems, (Russ), Nauka Publ. House, Moscow, pp. 60 (1984)
[25]M. Lasocka, Materials Science and Engineering**23**, 173 (1976);10.1016/0025-5416(76)90189-0
[26]K.O. Čajko, S.R. Lukić-Petrović, G.R. Štrbac, T.B. Ivetić,Acta Physica Polonica A, **129**(4), 509 (2016);10.12693/APhysPolA.129.509
[27]V. Mastelaro, S. Benazeth, H. Dexpert, A. Ibanez, R. Ollitrault-Fichet, Journal of Non-Crystalline Solids**151**(1–2), 1 (1992);10.1016/0022-3093(92)90003-3
[28]A. Kumar, P.B. Barman, R. Sharma,Journal of Thermal Analysis and Calorimetry 114(3), 1003 (2013);10.1007/s10973-013-3055-x
[29]V.M. Gorbachev, Journal of Thermal Analysis and Calorimetry**8**, 349 (1975);10.1007/BF01904012